

Study of intra-hour direct normal irradiance variability effects on hourly WRF-Chem outputs

Daniel Perez-Astudillo¹, Dunia Bachour¹ and Christos Fountoukis¹

¹ Qatar Environment and Energy Research Institute, HBKU, Doha (Qatar)

Abstract

Reliable and accurate solar resource information can be obtained, ideally, through direct ground measurements of the incoming solar irradiance; however, greater temporal and spatial coverages require most of the time some sort of modelling, commonly by directly deriving irradiance from satellite imaging or through physical, empirical, or numerical models. Operationally running the Weather Research and Forecasting (WRF) model provides the current values of irradiance as well as forecasts up to a few days ahead, and great efforts are being made to reduce the relatively high uncertainties from these models. While NWP models can provide forecasts at hourly intervals, which is relatively high for some applications, for solar radiation applications this temporal resolution cannot correctly capture the intra-hour variability and can be a source of errors especially during changing atmospheric conditions, in which hourly averages do not necessarily reflect representative enough conditions, particularly in the case of direct (or beam) normal irradiance, which is especially sensitive to clouds and aerosols. A study is presented here on the effects of intra-hour (within the hour) variability of beam radiation for cloud- and aerosol-variable conditions, in the use of hourly values in the advanced WRF-Chem model to predict beam irradiances in desert conditions.

Keywords: WRF-Chem, direct normal irradiance, solar irradiance variability

1. Introduction

Numerical weather prediction (NWP) models are useful tools not only for “traditional” meteorological applications, but also, increasingly, for solar resource applications. The NWP outputs, either as forecasts or modelling of cloudiness, directly impact the modelled solar radiation at ground level, and NWPs are also able to model and forecast solar irradiance, although usually with high uncertainties. The inclusion of better aerosol and aerosol transport treatment, for instance in the WRF-Chem model, in which recent advances have explored improvements in the modelling of global horizontal irradiance (G) and beam or direct normal irradiance (Gb), the latter a more challenging component of solar radiation given its high sensitivity to not only clouds but also (even in clear-sky, or cloudless, conditions) aerosols.

Apart from aerosol treatment, an additional source of uncertainty in the modelling is the temporal variability of solar radiation. Meteorological parameters such as air temperature, barometric pressure and relative humidity are typically not highly variable over short periods of time, and modelling at hourly resolutions is sufficient in most cases; accordingly, NWP outputs are obtained at hourly resolutions. Solar radiation, on the other hand, can vary even within few seconds, especially in cloudy conditions, and changes are even larger in Gb, for which even a small passing cloud reduces Gb to zero during the time the sun is behind the cloud; similarly, varying aerosols have a large effect on Gb. High-resolution ground Gb measurements are commonly collected as 1-minute averages of higher-frequency samples, and as such are able to capture a more realistic picture of Gb; when these are averaged over one hour and compared to hourly averages from the WRF model, the latter have the disadvantage of missing those details. In this work, we present a study of the effect, on WRF-Chem model (Fast et al, 2005) results, of the variability of Gb within hourly intervals in a mostly cloudless location, but with high and variable aerosol loads (mainly due to airborne desert dust); cloudy and cloudless skies are included in order to try to identify the effects of aerosols. The hourly averages of ground-measured Gb are compared to the corresponding outputs from the WRF-Chem model as a function of the variability of the ground-measured 1-minute Gb values within the hour.

2. Methodology

The site of this study is Doha, Qatar (25° N, 51° E), namely a desert location, in which clear skies are the common conditions, but with periods of cloudiness and rain during winter and occasionally scattered throughout the year. Airborne desert sand is, however, present throughout the year, with frequent sandstorms especially around summer months, when temperature and humidity also increase.

Direct normal irradiance is measured at this site with a high-quality monitoring station equipped with a Kipp and Zonen CHP-1 pyrheliometer mounted on a sun tracker, which also hosts two pyranometers measuring global horizontal and (with a shading assembly) diffuse horizontal irradiances (G and G_d , respectively). These irradiances are sampled every second and the 1-minute averages are saved. Since these 3 components are available, BSRN quality checks (Long and Dutton, 2010) are applied to filter the 1-minute G_b data used here for studying variability and for averaging over each hour.

A three-dimensional atmospheric meteorology-chemistry model, namely WRF-Chem, with a triple-nesting configuration over the region of interest, focusing particularly on the hot desert climate, is employed here to simulate G_b , considering an advanced treatment of aerosols.

Several metrics are explored to characterise the variability of G_b within each hour:

- Range (difference between the maximum and minimum values within the interval).
- Standard deviation.
- Inter-quartile range, IQR (range of the middle half of the data --Q1 to Q3-- in the interval).

To obtain the inter-quartile range, or IQR, the (ground-measured) 1-minute G_b values within each hour are first sorted by G_b and divided into quartiles; note that, in this study, a minimum of 5 usable minutes (passing quality checks and with $SZA < 90$ deg) were required within each hour in order to assign an IQR. Q1 is the lower quartile or 25th percentile, Q2 is the median or 50th percentile, and Q3 is the upper quartile or 75th percentile. Then,

$$IQR = Q3 - Q1 \quad (\text{eq. 1})$$

In addition, the clearness index K_t and the sun's zenith angle SZA are obtained for each of the hours included in this study. K_t is defined as:

$$K_t = \frac{G}{G_{TOA}} \quad (\text{eq. 2})$$

where G_{TOA} is the extra-terrestrial, or top-of-the-atmosphere, global horizontal irradiance, that is, the light coming from the sun, projected on a horizontal plane, before crossing the earth's atmosphere. The clearness index provides an indication on the cloudiness at the considered instant or interval; however, there is no wide consensus yet as to an objective definition of clear-skies (see e.g. Ruiz-Arias and Gueymard, 2023, and references therein). The sun's zenith angle is measured from the vertical overhead, corresponding to 0 degrees, with the horizontal corresponding to 90 degrees, and is calculated here using an implementation of NREL's SolPos v.2 algorithm (NREL, 2001).

The differences between (time-) coincident pairs of hourly values of measured and WRF-Chem-modelled G_b are analysed in the following section, as function of K_t , SZA and of the variability metrics listed above, for all daytime hours, i.e. hours in which average $SZA < 90$ degrees. Note that in Figures 2 to 7 the (hourly) data are presented binned in x and y , and the colour scales on the right side denote the number of (hourly) entries within each bin.

3. Results

3.1. Selected data

Data from four months are studied here. These months are May, July and August 2022, and February 2023. These cover different sky conditions throughout the year, from winter to summer, and days with sunny, cloudy

and dusty conditions, resulting in a good variety of both smooth and variable solar conditions. Note that in all figures, the months are shown in order from February to August, to reflect winter to summer progression, although the included February corresponds to the calendar year after that of the other months.

3.2. Hourly beam irradiance

For a general view on the measured and modelled values, Figure 1 shows the profiles of hourly Gb, from both sources, throughout the four months; Figure 2 shows the same data in scatter plots, in bins of 10 W/m². Gb is very sensitive to atmospheric conditions, mainly clouds and aerosols, to a higher degree than global irradiance; therefore, relatively larger dispersions are commonly seen in comparisons of measured and modelled (not only physical models like WRF but also from satellite-based models) Gb.

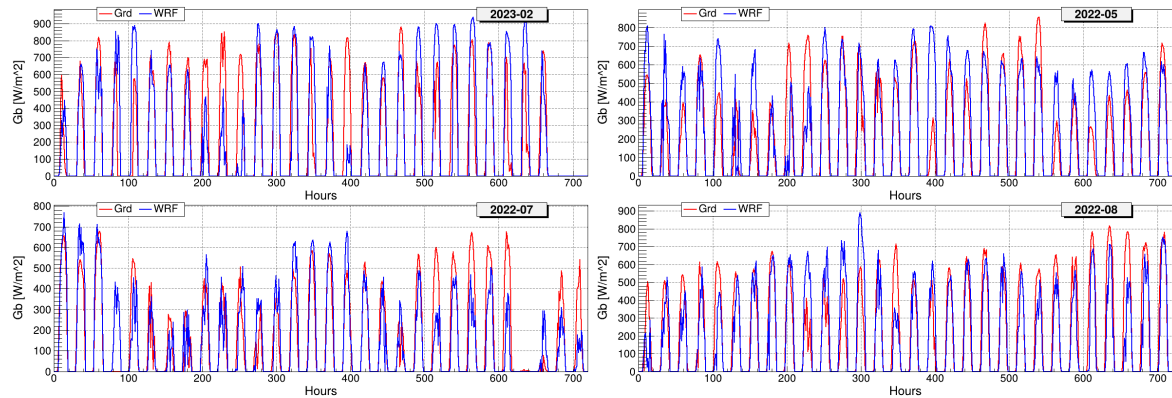


Fig. 1: Daily profiles of (red) measured and (blue) modelled hourly Gb in the studied months.

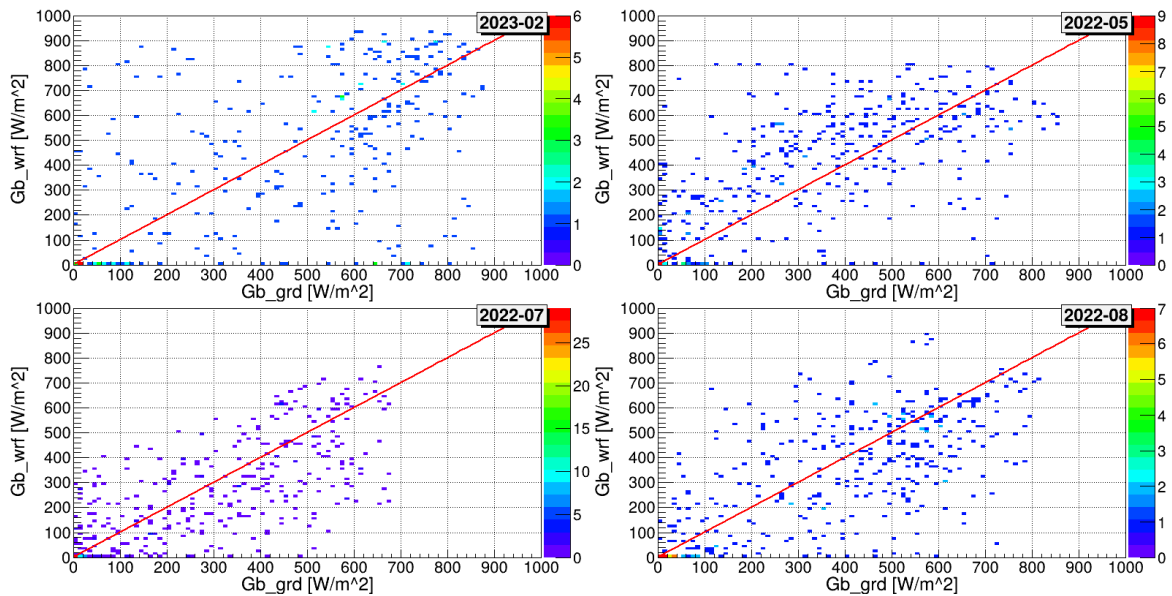


Fig. 2: Comparison of measured (x-axis) and modelled (y-axis) hourly Gb in the studied months. The colour scales indicate the number of entries in each bin (10 W/m² in both x and y).

3.3 Differences as function of clearness index and of sun zenith angle

Figure 3 shows the differences in WRF-Chem-modelled to ground-measured Gb as function of SZA for all daytime hours (SZA<90) of the considered months. Note that in February for this location the SZA does not go below 30 degrees at any hourly average (in other words, hourly averages of solar elevation stay below 60 degrees above the horizon). Somewhat larger differences can be seen around mid-elevations but on average there is no clear dependency on SZA.

The differences as function of Kt are shown in Figure 4. It can be seen that WRF-Chem tends to underestimate

Gb at the higher clearness values, from around 0.6-0.7 on. This suggests that WRF-Chem works better under cloudy skies than under clear skies, which may seem counterintuitive, but can be understood by noting the influence of high aerosol loads in the region, which affect Gb more clearly in the absence of clouds, indicating the need for a better inclusion of aerosols in WRF-Chem.

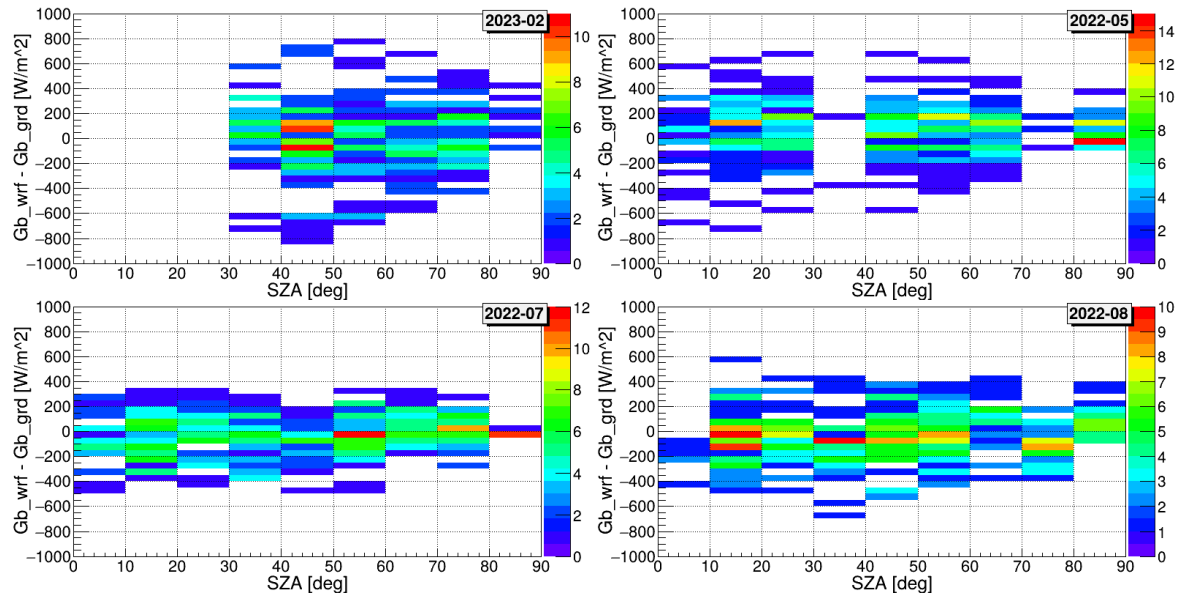


Fig. 3: Differences in Gb as function of solar zenith angle, per month.

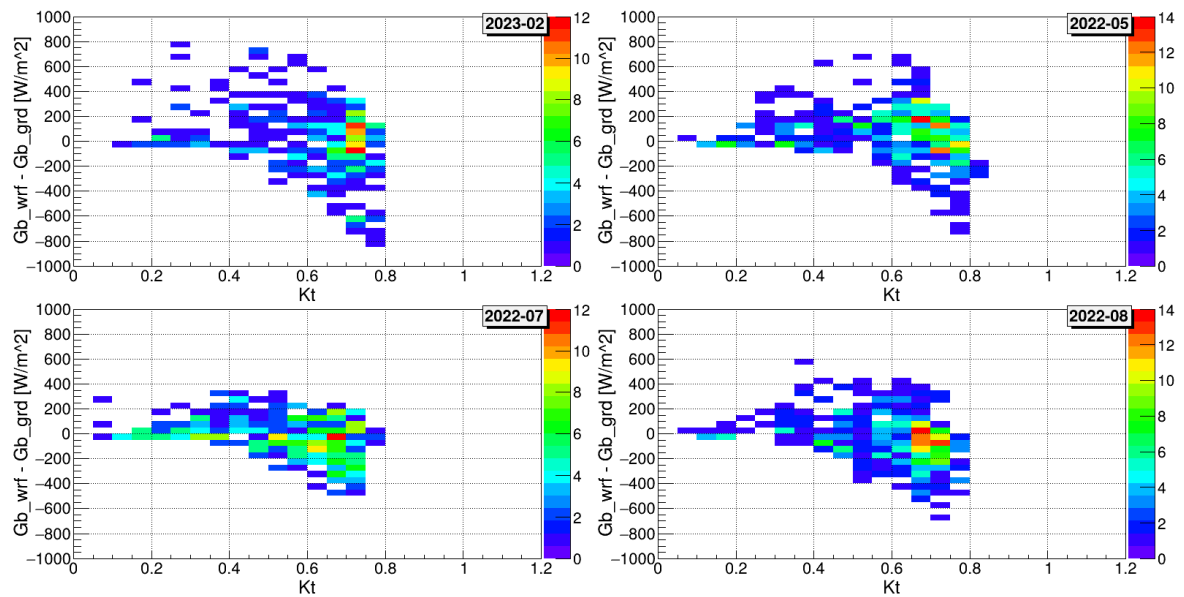


Fig. 4: Differences in Gb as function of clearness index, per month.

3.4 Differences by variability

In order to look for model deviations due to intra-hour variability, Figures 5, 6 and 7 show the model-to-measurement differences in Gb as function of the range, standard deviation and inter-quartile range, respectively, of the 1-minute measured Gb within the hour (see definitions in Section 2).

Comparing the spread of data along the x-axis across the months, larger variations in Gb can be found, as expected, in February, due to increased cloudiness and unstable weather during winter in Qatar. Along the y-axis, the differences between WRF-Chem and measurements appear generally less widespread in summer, particularly in July, and a dependency on the variability metrics (x-axis) is not clear, although an indication

towards overestimation can be seen at higher variabilities during August; a possible explanation for this overestimation could be too few shallow convection clouds in the WRF-Chem simulation.

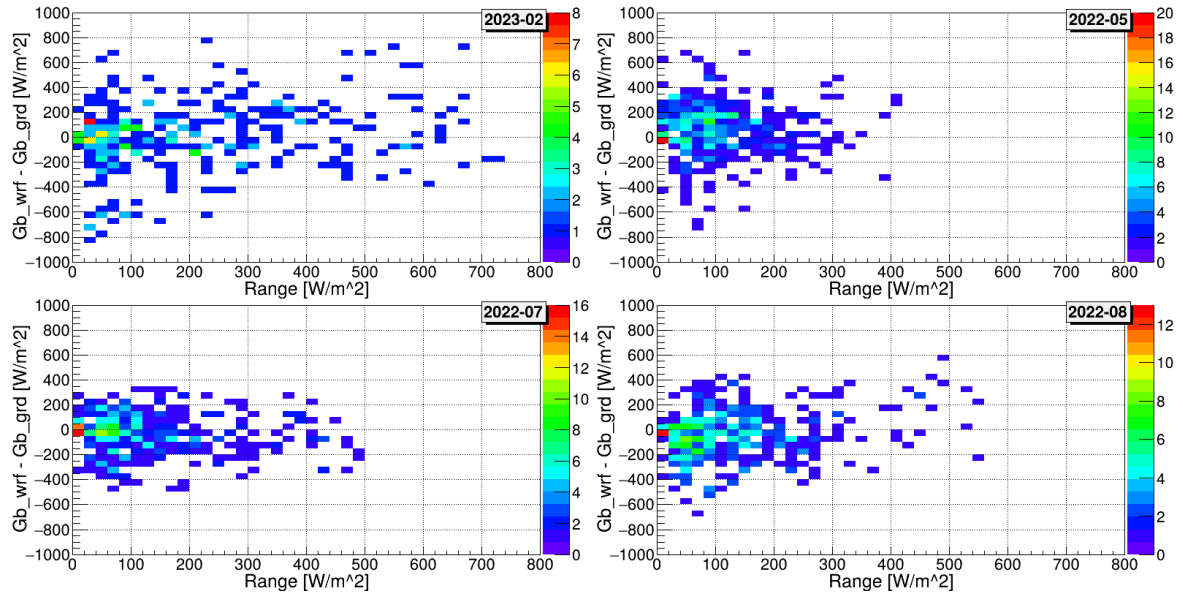


Fig. 5: Differences in Gb as function of the range of 1-min Gb within the hour, per month.

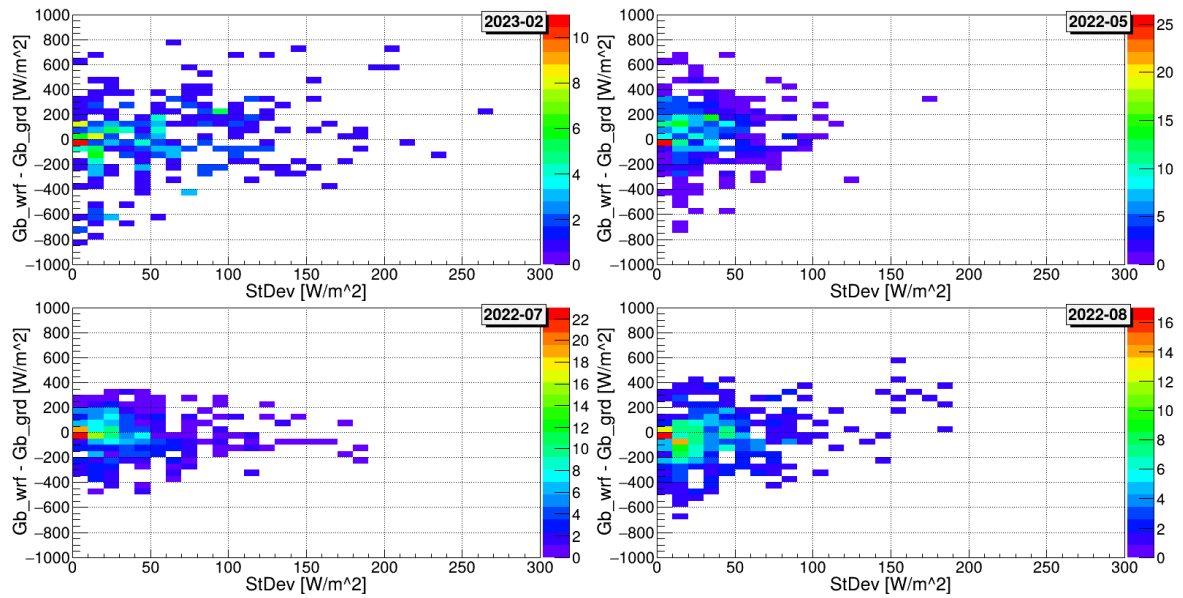


Fig. 6: Differences in Gb as function of the standard deviation of 1-min Gb within the hour, per month.

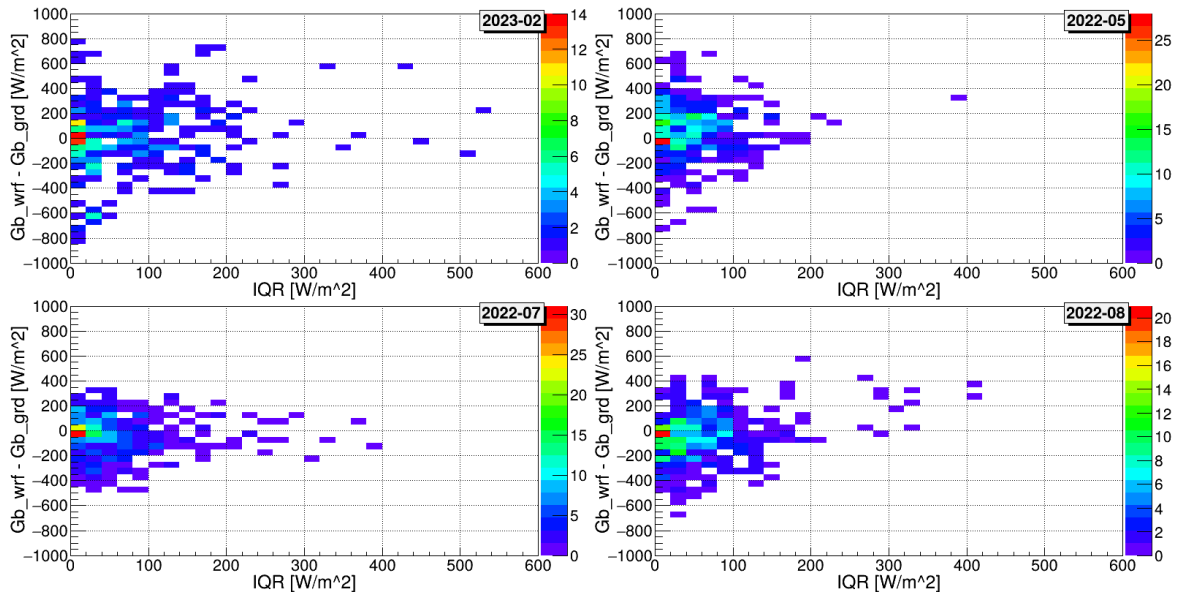


Fig. 7: Differences in Gb as function of the inter-quartile range of 1-min Gb within the hour, per month.

To provide a clearer view on any dependencies, Figures 8, 9 and 10 show the same variables as Figures 5, 6 and 7, namely difference in hourly modelled vs measured Gb as function of range, standard deviation and IQR of the 1-minute ground measurements, respectively, but presented in a different form. The points, which represent the averages along the y-axis for each x-axis bin, are shown with standard errors (standard deviation divided by \sqrt{n} ; for the n 1-hour entries along the y-axis on that x-axis bin). From these figures, the increased overestimation in WRF-Chem Gb, i.e. positive differences, is more clearly seen at the higher values of variability, especially at higher standard deviation and IQR values and more notably in August. On the other hand, underestimation of Gb can be seen throughout but seems more prevalent than overestimation at low variabilities.

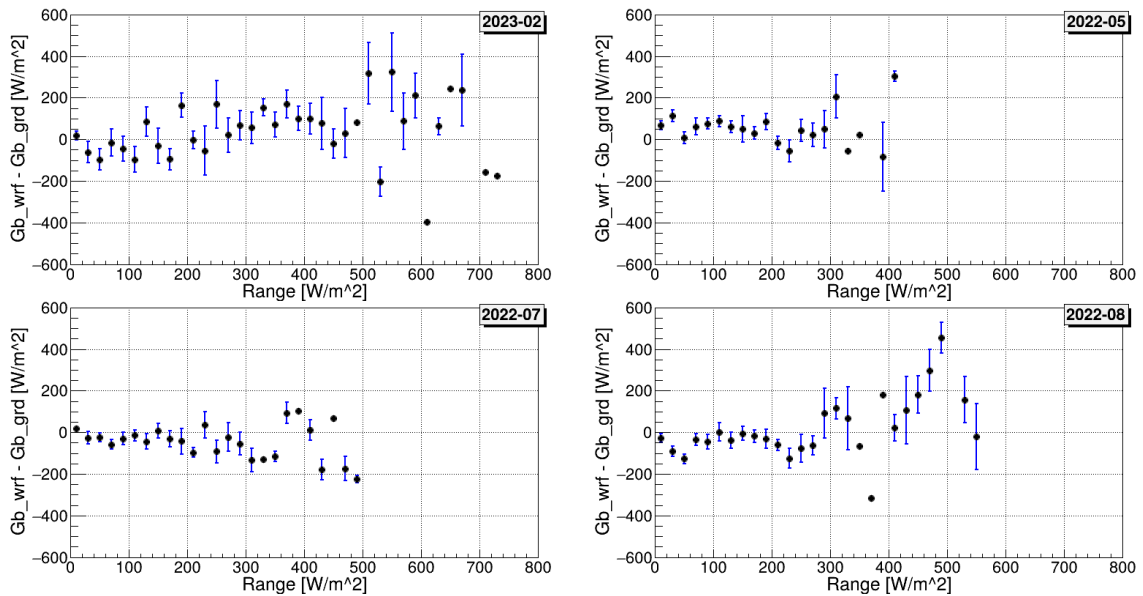


Fig. 8: Means and std error of differences in Gb as function of the range of 1-min Gb within the hour, per month.

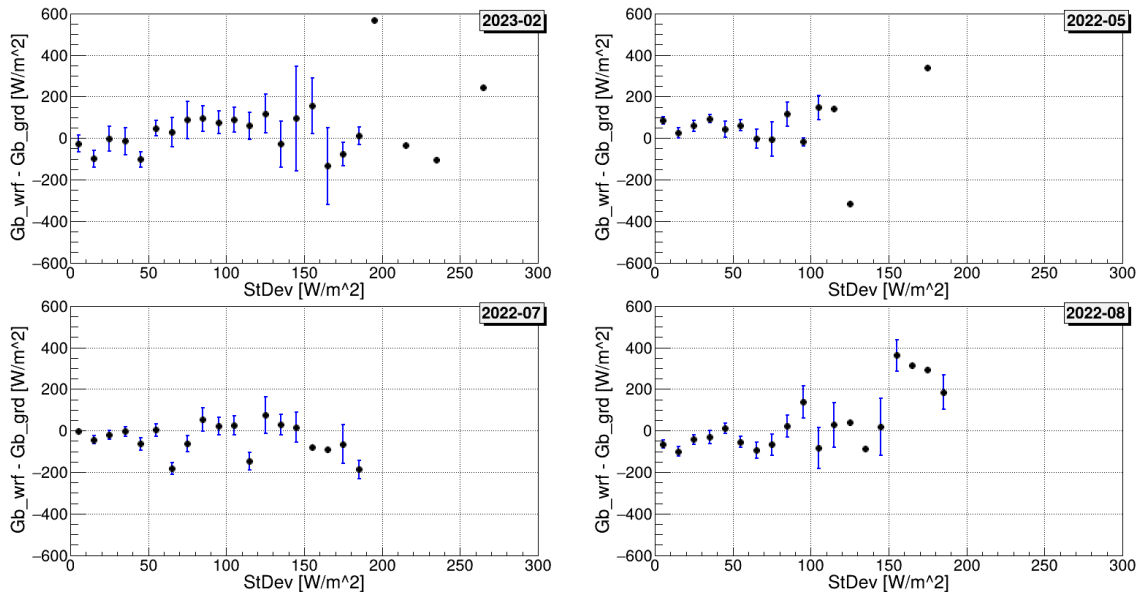


Fig. 9: Means and std error of differences in Gb as function of the standard deviation of 1-min Gb within the hour, per month.

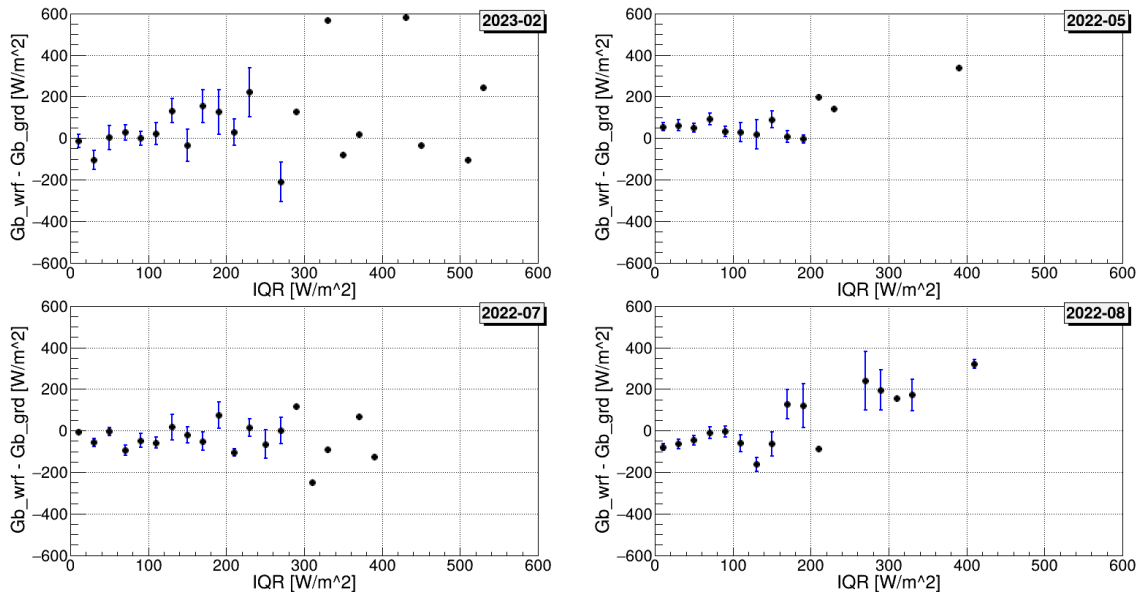


Fig. 10: Means and std error of differences in Gb as function of the inter-quartile range of 1-min Gb within the hour, per month.

4. Conclusions

Numerical weather prediction models, such as WRF, are valuable tools to obtain insight not only on meteorological information, but also on solar resources at ground level. Beam or direct irradiance is particularly challenging for models, given its high sensitivity to most atmospheric components, from clouds (as the case of global irradiance) to aerosols (which affect global irradiance to a smaller degree). As aerosol measurements are generally scarce, models using this information (from WRF to satellite models for solar irradiance) have higher uncertainty in the derivation of direct than for global irradiance. An additional complication is the usually high temporal variability of atmospheric aerosol contents, with even higher impact in regions, such as deserts, with large aerosol loads; WRF models work with comparatively larger temporal resolutions (hourly or three-hourly), which may not be able to capture these rapid changes, further increasing uncertainty. The study presented here covers 4 months with varying sky conditions, from winter to summer, sunny to rainy and dusty, in a desertic location, and shows that the WRF-Chem model, at hourly level, results in higher errors in direct irradiance, as compared to the corresponding ground measurements, when the

cloudiness is lower (indicating the effect of aerosols on solar radiation) and at high irradiance variabilities (based on the 1-minute ground measurements), mainly as measured through the standard deviation and the inter-quartile range of the 1-minute measurements within each hour. These results underline a need for a better treatment of aerosol inputs in the model, which currently can be summarised in two limitations: the temporal resolution of the aerosol inputs (usually only one or a couple of values per day are available), and the processing of the aerosols in the model itself; these shortcomings are currently being addressed in WRF-Chem by additional research at QEERI.

5. Acknowledgments

Research reported in this work was supported by the Qatar Research Development and Innovation Council (Grant: ARG01-0503-230061). The content is solely the responsibility of the authors and does not necessarily represent the official views of Qatar Research Development and Innovation Council.

6. References

- Fast, L.D., Gustafson, Jr. W. I., Easter, R.C., Zaveri, R.A., Barnard, J.C., Chapman, E.G., Grell, G.A., 2005. Evolution of ozone, particulates, and aerosol direct forcing in an urban area using a new fully-coupled meteorology, chemistry, and aerosol model, *J. Geophys. Res.* (111), D21305. doi:10.1029/2005JD006721
- Long, C.N., Dutton, E.G. 2010. Available online at https://epic.awi.de/id/eprint/30083/1/BSRN_recommended_QC_tests_V2.pdf (last accessed 7/Aug/2024).
- NREL, 2001. The code, references, and an online calculator are available at <https://www.nrel.gov/grid/solar-resource/solpos.html> (last accessed 7/Aug/2024).
- Ruiz-Arias, J.A., Gueymard, C.A., 2023. CAELUS: Classification of sky conditions from 1-min time series of global solar irradiance using variability indices and dynamic thresholds. *Solar Energy* 263, 111895. DOI: 10.1016/j.solener.2023.111895